PCCP

PAPER

View Article Online
View Journal | View Issue

Cite this: *Phys. Chem. Chem. Phys.*, 2018, **20**, 24665

Unexpected stable phases of tungsten borides†

Changming Zhao,[a] Yifeng Duan,*[a] Jie Gao,[a] Wenjie Liu,[a] Haiming Dong,[a] Huafeng Dong,*[b] Dekun Zhang[c] and Artem R. Oganov*[def]

Received 4th July 2018,
Accepted 7th September 2018

DOI: 10.1039/c8cp04222e

rsc.li/pccp

Tungsten borides are a unique class of compounds with excellent mechanical properties comparable to those of traditional superhard materials. However, the in-depth understanding of these compounds is hindered by the uncertainty of their phase relations and complex crystal structures. Here, we explored the W–B system systematically by *ab initio* variable-composition evolutionary simulations at pressures from 0 to 40 GPa. Our calculations successfully found all known stable compounds and discovered two novel stable phases, $P\bar{4}2_1m$-WB and $P2_1/m$-W_2B_3, and three nearly stable phases, $R3m$-W_2B_5, $Ama2$-W_6B_5, and $Pmmn$-WB_5, at ambient pressure and zero Kelvin. Interestingly, $P\bar{4}2_1m$-WB is much harder than the known α and β phases, while $Pmmn$-WB_5 exhibits the highest hardness. Furthermore, it is revealed that the much debated WB_4 becomes stable as the $P6_3/mmc$ (2 f.u. per unit cell) phase at pressures above ~1 GPa, not at ambient pressure as reported previously. Our findings provide important insights for understanding the rich and complex crystal structures of tungsten borides, and indicate WB_2, WB_4, and WB_5 as compounds with the most interesting mechanical properties.

1 Introduction

Superhard materials are of great industrial importance and have a wide range of applications, for example, in cutting and polishing tools, and as coatings and abrasives.[1] However, typical superhard materials,[2,3] such as diamond and cubic-BN,[4] are synthesized at high pressure, which makes them expensive. However, in recent years, transition-metal light-element compounds (OsB_2, CrB_4, CrN, WB_4, *etc.*[5–12]) have attracted interest because of their excellent mechanical properties and synthesis without the need of high pressure.

Among these compounds, the W–B system is one of the most widely investigated,[10,13,14] because it has been demonstrated to exhibit superior mechanical properties, high chemical inertness and high electronic conductivity.[7,15] Experimentally, six different stoichiometric compositions, W_2B,[16] WB,[16,17] WB_2,[18] W_2B_5,[16] WB_3,[11,12] and WB_4,[14,15] have been synthesized. However, common issues in the ambiguity of crystal structures still remain in tungsten borides. Because of the weak scattering of X-rays by boron atoms, only the positions of tungsten atoms can be directly determined by X-ray diffraction, creating an uncertainty in the tungsten boride architecture. WB_4, the material with the highest B content, is one of the most promising candidates as a superhard material among the transition-metal/light-element compounds, and the measured hardness is very high (43.3 ± 2.9 GPa)[15] compared to that of c-BN. However, recent studies suggested that the widely accepted $P6_3/mmc$-$4u$-WB_4 (nu denotes that the structure contains n formula units per unit cell) is unstable, and the synthesized material should be $P6_3/mmc$-WB_3[19,20] or WB_{3+x} ($x < 0.5$),[11] which has subsequently been verified by their X-ray diffraction, phonon stability and ideal strength results. Furthermore, recent experiments showed no signs of the formation of WB_4.[11,12] Moreover, it was argued that the earlier established W_2B_5 should be W_2B_4.[21] Therefore, we want to establish whether there are stable structures for WB_4 or W_2B_5. On the other hand, the rich phase diagrams lead to another issue: Are there new stable structures of the W–B system, in particular, for the chemical composition that has never been checked? Therefore, it is highly desirable to explore in detail the crystal structures of the W–B compounds and to provide essential guidance in synthesizing new superhard tungsten boride materials.

In this work, we have systematically investigated the crystal structures in the W–B system by combining density functional theory (DFT) and *ab initio* evolutionary algorithm USPEX,[22–24]

[a] *School of Physics, China University of Mining and Technology, Xuzhou, Jiangsu 221116, China. E-mail: yifeng@cumt.edu.cn*
[b] *School of Physics and Optoelectronic Engineering, Guangdong University of Technology, Guangzhou, Guangdong 510006, China. E-mail: hfdong@gdut.edu.cn*
[c] *School of Materials Science and Engineering, China University of Mining and Technology, Xuzhou, Jiangsu 221116, China*
[d] *Skolkovo Institute of Science and Technology, Skolkovo Innovation Center, 3 Nobel St., Moscow 143026, Russia. E-mail: a.oganov@skoltech.ru*
[e] *Moscow Institute of Physics and Technology, 9 Institutskiy Lane, Dolgoprudny city, Moscow Region 141700, Russia*
[f] *International Center for Materials Discovery, Northwestern Polytechnical University, Xi'an 710072, China*

† Electronic supplementary information (ESI) available: Structural parameters and elastic constants for the W–B system. See DOI: 10.1039/c8cp04222e

which has successfully predicted the structures of various systems.[25–27] First, we carried out variable-composition calculations at pressures of 1 atm, 10, 20, 30 and 40 GPa to find novel compounds and structures. Then, for each of these compositions, we performed fixed-composition calculations with different numbers of formula units at different pressures. Two stable phases, $P\bar{4}2_1m$-WB and $P2_1/m$-W_2B_3, and three low-enthalpy metastable phases, *Ama*2-W_6B_5, $R3m$-W_2B_5, and *Pmmn*-WB_5, were first discovered at ambient pressure. Moreover, we have obtained a complete pressure–composition phase diagram at 0–40 GPa and analyzed the hardness for all the phases.

2 Computational methods

DFT calculations were performed with the Perdew–Burke–Ernzerhof generalized gradient approximation[28] functional and the VASP code.[29,30] The electron–ion interaction was described by means of a projector augmented wave[31] with $5d^46s^2$ and $2s^22p^1$ treated as valence states for W and B, respectively. We used the plane wave cutoff energy of 550 eV, and we sampled the Brillouin zone with uniform Γ-centered meshes with a resolution of $2\pi \times 0.025$ Å^{-1} for subsequent highly precise relaxations and property calculations. The phonon dispersions were calculated using the PHONOPY package[32] and the hardness was computed using the Chen model.[33]

3 Results and discussion

Our structure search produced a large number of tungsten boride structures, whose enthalpies of formation, ΔH, were calculated per atom using $\Delta H(W_{1-x}B_x) = H(W_{1-x}B_x) - [(1-x)H(W) + xH(B)]$, where x is the concentration of B. For W, the known bcc structure is stable in the considered pressure range. For B, a phase transition from the α to γ phase takes place at ~19 GPa (Fig. S1, ESI†), in excellent agreement with the previous theoretical and experimental work.[25] The enthalpies of formation of the predicted structures at 1 atm, 20 GPa and 40 GPa are summarized in the convex hull diagrams shown in Fig. 1 and Fig. S2 (ESI†). A stable phase, by definition, has a lower enthalpy (or, more generally, Gibbs free energy) than any other phase or phase assemblage of the same composition, therefore, the convex hull is formed by stable phases, and only by them. Fig. 1(a) shows that there are five stable tungsten borides, $I4/m$-W_2B, $P\bar{4}2_1m$-WB, $P2_1/m$-W_2B_3, $P6_3/mmc$-2*u*-WB_2, and $R\bar{3}m$-WB_3, at ambient pressure, where $I4/m$-W_2B, $P6_3/mmc$-2*u*-WB_2 and $R\bar{3}m$-WB_3 are consistent with the reported results,[10,11,19] and $P\bar{4}2_1m$-WB and $P2_1/m$-W_2B_3 are novel structures that we found. When pressure reaches 20 GPa, the stable phases become $I4/m$-W_2B, $I4_1/amd$-WB, $R\bar{3}m$-WB_2, and $P6_3/mmc$-2*u*-WB_4 (Fig. 1(b)), which remain stable at least until 40 GPa (Fig. S2, ESI†). This indicates that pressure can change the stability of such low-compressibility compounds and thus generate new stable structures. The phonon dispersion curves (Fig. 2) and elastic constants (Table S2, ESI†) computed at ambient pressure indicate that all phases satisfy the dynamical and mechanical stability criteria.

Monoboride WB has been reported to exist in two phases: the low-temperature tetragonal α-WB phase (Fig. 2(b)) and the high-temperature orthorhombic β-WB phase (Fig. 2(c))[16,17] with space groups $I4_1/amd$ and *Cmcm*, respectively. Surprisingly, we find that our predicted $P\bar{4}2_1m$-WB (Fig. 2(a)) is more energetically stable than the above two structures at ambient pressure, and thus it is the ground state. The newly predicted tetragonal $P\bar{4}2_1m$ phase, which has two types of boron atoms at the Wyckoff 4e and 2c positions (Table 1), is structurally very different from the α and β phases, as shown in Fig. 2(a–c). The boron atom at 2c is eight-coordinate, bonded to six tungsten atoms at distances of 2.311 (four) and 2.326 (two) Å, and two boron atoms at 1.838 Å, while a boron atom at 4e is also eight-coordinate, with seven tungsten atoms at distances

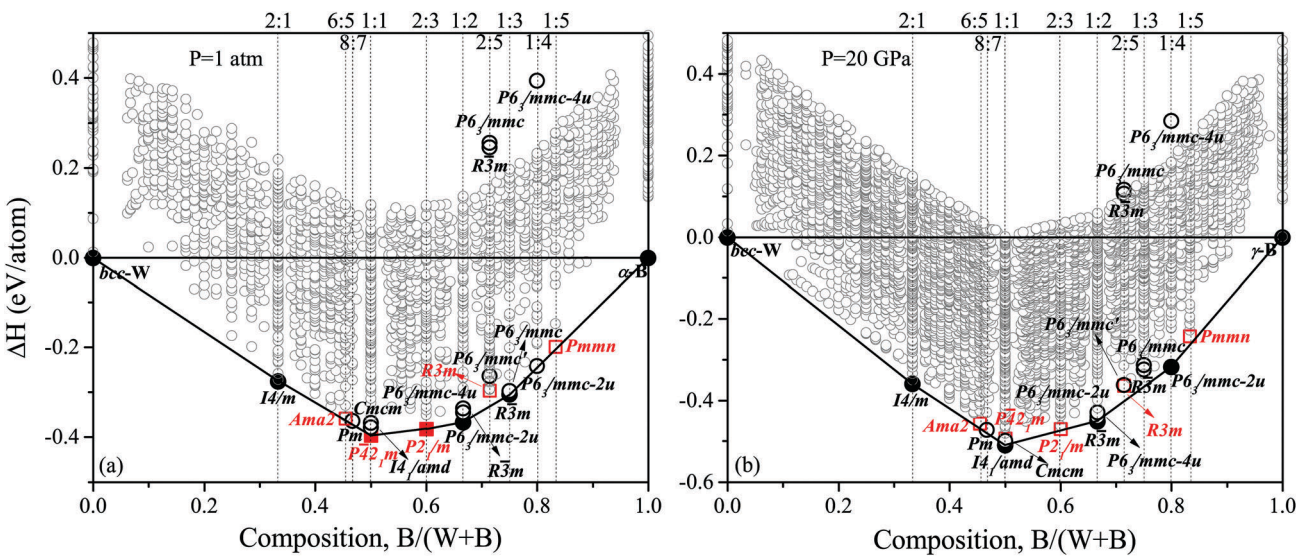

Fig. 1 Thermodynamic convex hulls of the W–B system predicted by our structure search at 1 atm and 20 GPa. Solid circles and squares denote stable phases and red ones (squares) denote the phases we first discovered. More structural details are listed in Table 1 and Table S1 (ESI†).

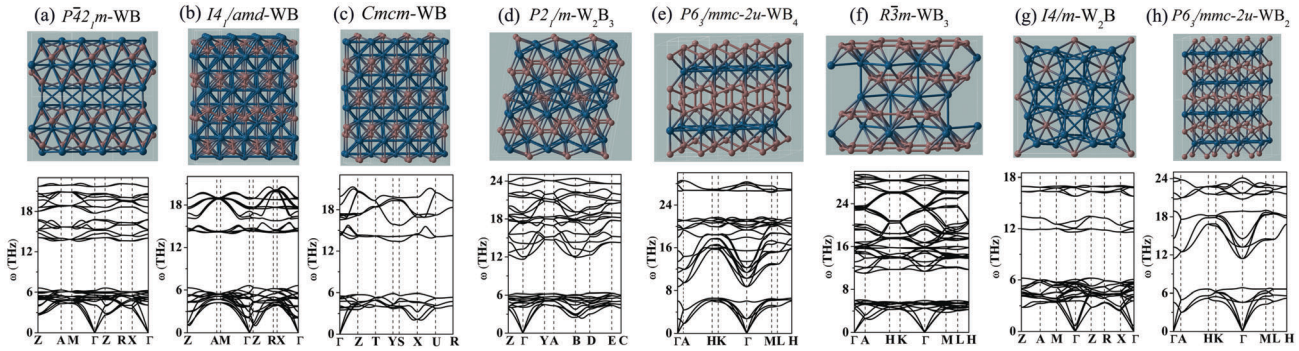

Fig. 2 Crystal structures and phonon dispersion curves for $W_{1-x}B_x$ at ambient pressure: (a) $P\bar{4}2_1m$-WB, (b) $I4_1/amd$(α)-WB, (c) $Cmcm$(β)-WB, (d) $P2_1/m$-W_2B_3, (e) $P6_3/mmc$-2u-WB_4, (f) $R\bar{3}m$-WB_3, (g) $I4/m$-W_2B and (h) $P6_3/mmc$-2u-WB_2. The large (blue) and small (pink) spheres represent W and B atoms, respectively. More structural details are listed in Table 1 and Table S1 (ESI†).

Table 1 Crystal structures of the predicted tungsten borides at ambient pressure

	Structure	Parameters (Å, °)	Atom	x	y	z
WB	$P\bar{4}2_1m$	$a = b = 4.3362$	W(4e)	0.7541	0.2541	0.1313
		$c = 6.8604$	W(2b)	0.0	0.0	0.5
			B(4e)	0.7529	0.7470	0.2393
			B(2c)	0.5	0.0	0.3830
W_2B_3	$P2_1/m$	$a = 4.5943$	W(2e)	0.1954	0.75	0.2773
		$b = 3.0128$	W(2e)	0.6545	0.25	0.1404
		$c = 7.2794$	B(2e)	0.8882	0.75	0.9745
		$\beta = 99.2735$	B(2e)	0.9262	0.25	0.4337
			B(2e)	0.5401	0.25	0.4341
W_2B_5	$R3m$	$a = b = 2.9225$	W(3a)	0.6667	0.3333	0.9812
		$c = 25.9018$	W(3a)	0.6667	0.3333	0.1659
			B(3a)	0.6667	0.3333	0.0742
			B(3a)	0.6667	0.3333	0.2525
			B(3a)	0.3333	0.6667	0.0422
			B(3a)	0.3333	0.6667	0.1049
			B(3a)	0.3333	0.6667	0.2273
W_6B_5	$Ama2$	$a = 6.1282$	W(8c)	0.9973	0.3298	0.4698
		$b = 9.4050$	W(4a)	0.0	0.0	0.4705
		$c = 8.5015$	W(4b)	0.75	0.1658	0.6779
			W(4b)	0.75	0.0024	0.1784
			B(8c)	0.9963	0.1658	0.2650
			B(4b)	0.75	0.4986	0.3884
			B(4a)	0.5	0.0	0.7661
			B(4b)	0.25	0.1629	0.3843
WB_5	$Pmmn$	$a = 6.3687$	W(2b)	0.5	0.0	0.9180
		$b = 5.1996$	W(2a)	0.5	0.5	0.7518
		$c = 8.9930$	W(2a)	0.0	0.0	0.5883
			B(8g)	0.7563	0.6690	0.9156
			B(8g)	0.7515	0.1671	0.7515
			B(8g)	0.7563	0.3351	0.5820
			B(4e)	0.0	0.3189	0.8078
			B(2b)	0.0	0.5	0.6284

of 2.261 (two), 2.319 (two), 2.356 (two) and 2.548 (one) Å, and one boron at 1.838 Å. Meanwhile, the α and β phases are structurally similar, and both have only one boron site with ninefold coordination composed by seven tungsten atoms and two boron atoms, and the bond distances of W–B (2.325 (four), 2.349 (two) and 2.491 (one) Å) and B–B (1.892 Å) in the α phase are very close to those of W–B (2.331 (four), 2.364 (two) and 2.491 (one) Å) and B–B (1.866 Å) in the β phase. The average W–B bond length of the $P\bar{4}2_1m$ phase is smaller than that of the α and β phases at ambient pressure, and thus bonding between the W and B atoms in the $P\bar{4}2_1m$ phase is stronger. This can be linked to $P\bar{4}2_1m$-WB having higher shear moduli, Young's moduli and hardness than the α and β phases (Table 2). The convex hull diagram at 20 GPa shows that the α phase has the lowest enthalpy, as shown in Fig. 1(b), while the enthalpy calculation reveals that a phase transition from $P\bar{4}2_1m$ to α occurs at ~11 GPa (Fig. S3(b), ESI†). On the other hand, the lower energy of $P\bar{4}2_1m$-WB results in the previously reported ground-state Pm-W_8B_7[11] being actually metastable, see Fig. 1(a).

The phase with stoichiometry W_2B_3 has never been reported, however, our search discovered a novel monoclinic structure with the space group $P2_1/m$ that lies on the convex hull (Fig. 1(a)), which indicates that it is thermodynamically stable. By closely examining the structural details of this new phase, as illustrated in Fig. 2(d), we find that the boron atoms are divided into two types: one type forms zigzag chains along the [010] direction, while the other forms a puckered graphene-like layer. The tungsten atoms form hexagonal networks surrounding the zigzag boron chains, which is similar to the structure of β-WB.

Table 2 Bulk modulus B (GPa), shear modulus G (GPa), Young's modulus E (GPa), Poisson's ratio ν and Vickers hardness H_v (GPa) of $W_{1-x}B_x$ at ambient pressure

	Structure	B	G	E	ν	H_v	H_v (ref.)
W_2B	$I4/m$	341	171	439	0.286	15.0	14.2[a]
W_6B_5	$Ama2$	344	210	523	0.247	22.6	
W_8B_7	Pm	347	206	515	0.252	21.5	19.6[b]
WB	$P\bar{4}2_1m$	344	247	598	0.210	31.2	
	$I4_1/amd$	355	211	528	0.252	21.9	21.5[a]
	$Cmcm$	353	195	495	0.267	18.9	18.0[c]
W_2B_3	$P2_1/m$	333	244	589	0.205	31.7	
WB_2	$P6_3/mmc$-2u	320	276	643	0.165	42.1	41.3[a]
	$R\bar{3}m$	330	245	589	0.203	32.2	32.4[a]
W_2B_5	$R3m$	312	252	595	0.182	36.5	
WB_3	$R\bar{3}m$	296	251	587	0.170	38.8	35.9[b]
	$P6_3/mmc$	293	245	574	0.173	37.4	39.2[a]
WB_4	$P6_3/mmc$-2u	302	259	604	0.167	40.0	
WB_5	$Pmmn$	288	267	611	0.164	44.9	

[a] Ref. 35. [b] Ref. 11. [c] Ref. 34.

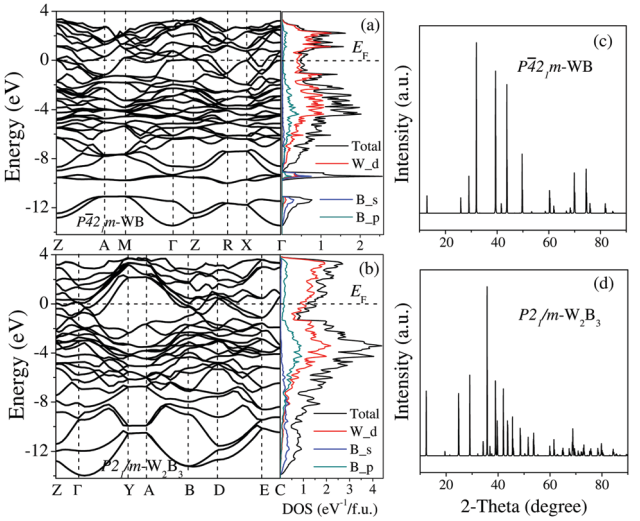

Fig. 3 Band structure and density of states (DOS) of (a) $P\bar{4}2_1m$-WB, and (b) $P2_1/m$-W_2B_3. E_F, Fermi energy. Computed X-ray diffraction (XRD) spectra of (c) $P\bar{4}2_1m$-WB and (d) $P2_1/m$-W_2B_3 (X-ray wavelength λ = 1.54056 Å).

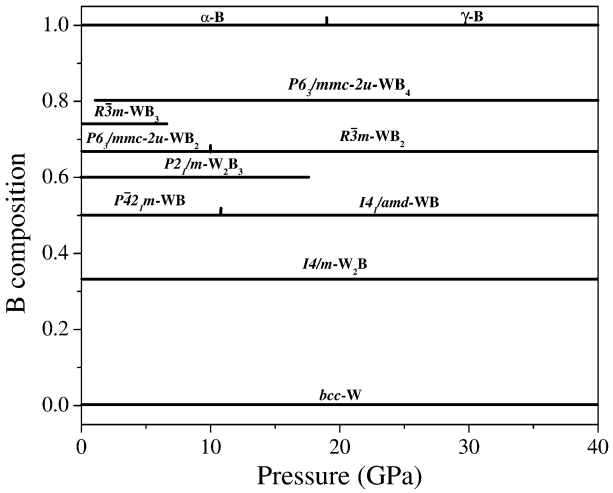

Fig. 4 Pressure–composition phase diagram of the W–B system.

The adjacent tungsten layers are isolated by one boron layer, forming a sandwich structure. By calculating the relative enthalpies, we find that $P2_1/m$-W_2B_3 remains stable at pressure up to ~18 GPa (Fig. S3(d), ESI†), and then becomes metastable with respect to α-WB and $R\bar{3}m$-WB_2.

Fig. 3 presents the calculated electronic band structures and density of states (DOS) of the $P\bar{4}2_1m$-WB and $P2_1/m$-W_2B_3 phases. The bands cross the Fermi level (E_F), indicating the metallic character of these two phases. The total DOS at the E_F comes mainly from the W 5d states, which is the principal cause for the metallicity. From the site-projected DOS of the two compounds, it is clear that the W 5d orbitals undergo strong hybridization with the B 2p orbitals, indicating the covalent bonding nature of W–B. We also computed the X-ray diffraction (XRD) patterns for $P\bar{4}2_1m$-WB and $P2_1/m$-W_2B_3, as shown in Fig. 3(c and d), which can be used to compare with the possible experimental results in the future.

WB_4 has attracted much attention due to its superior mechanical properties.[14,15] Our search shows that the $P6_3/mmc$-2u phase has the lowest enthalpy, in accordance with previous results,[10,11] but it is metastable at ambient pressure, *i.e.*, it lies above the convex hull, see Fig. 1(a). Surprisingly, Fig. 1(b) shows that $P6_3/mmc$-2u-WB_4 is stable, and WB_3 is metastable at 20 GPa. Our detailed calculations show the transition pressures are ~1 GPa and ~6 GPa for WB_4 and WB_3, respectively (Fig. S3(f and e), ESI†), which indicates that pressure can be used as a powerful tool to synthesize WB_4. Further calculations of phonon dispersions and elastic constants at ambient pressure (Fig. 2(h) and Table S2, ESI†) show that $P6_3/mmc$-2u-WB_4 is dynamically and mechanically stable. Therefore, this WB_4, synthesized under pressure, can exist under ambient conditions. The predicted lowest-enthalpy W_2B phase is $I4/m$, which coincides with the experimentally observed structure,[10] and it can remain stable up to 40 GPa (Fig. S3(a), ESI†). The predicted and experimentally observed ground-state $P6_3/mmc$-2u of WB_2 transforms into the $R\bar{3}m$ phase at ~10 GPa (Fig. S3(c), ESI†), in good agreement with the reported 9.2 GPa.[19] These detailed enthalpy calculations allow us to construct the pressure–composition phase diagram of the W–B system, which is depicted in Fig. 4.

Metastable structures are of great significance and can often be synthesized by choosing appropriate precursors and controlling conditions such as the quench rate. ε-W_2B_5, which was initially thought to have a hexagonal ($P6_3/mmc$) or rhombohedral ($R\bar{3}m$) structure,[16] was recently identified as WB_2 (denoted as W_2B_4).[21] Our search predicts that the lowest-enthalpy phase is rhombohedral $R3m$ (Fig. 5(a)), which is a metastable structure whose enthalpy of formation is slightly above the convex hull. The enthalpy of $R3m$-W_2B_5 is ~0.033 eV per atom lower than that of the recently predicted $P6_3/mmc'$-W_2B_5[10,34] at ambient pressure. Meanwhile, we also found two other low-enthalpy metastable phases, $Ama2$-W_6B_5 and $Pmmn$-WB_5 (Fig. 5(b and c)).

$Pmmn$-WB_5 has a remarkable structure, in which the boron atoms form a three-dimensional framework. In order to illustrate the bonding and mechanical properties of $Pmmn$-WB_5, the charge density distribution (Fig. 5(d)) and DOS (Fig. 5(e)) were calculated at ambient pressure. We can see that the 3D-framework is made of short and strong B–B bonds, with a large number of bonds per unit of volume and a high valence electron density, which are the key factors of superhardness. At the same time, this 3D boron framework resists shear deformation and hinders creation and motion of dislocations. The DOS near the E_F stems from the W 5d and B 2p states. It is noteworthy that the W 5d orbitals undergo significant hybridization with the B 2p orbitals, indicating strong covalent bonding between the W and B atoms. These factors explain the superhardness of $Pmmn$-WB_5.

Table 2 lists the bulk modulus, shear modulus, Young's modulus, Poisson's ratio and Vickers hardness of the above-mentioned structures. Calculated phonon dispersions and elastic constants (Fig. 2 and 4 and Table S2, ESI†) indicate that they are dynamically and mechanically stable at ambient pressure. Hardness is the biggest factor that stimulates interest

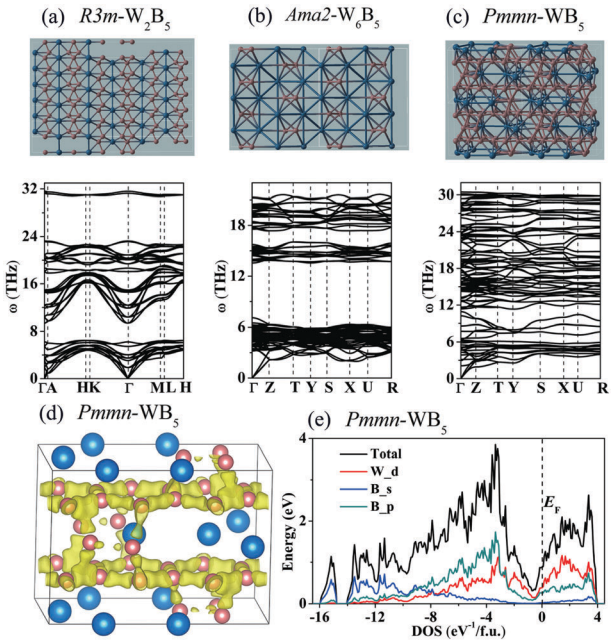

Fig. 5 Crystal structures and phonon dispersion curves for the predicted metastable $W_{1-x}B_x$ at ambient pressure: (a) $R3m$-W_2B_5, (b) $Ama2$-W_6B_5 and (c) $Pmmn$-WB_5. (d) Charge density distribution of $Pmmn$-WB_5. (e) Total and partial density of states of $Pmmn$-WB_5. E_F, Fermi energy. The large (blue) and small (pink) spheres represent the W and B atoms, respectively. More structural details are listed in Table 1.

in the W–B system. Our calculated hardness values of 21.9 GPa for α-WB and 18.9 GPa for β-WB agree well with the reported 21.5 and 19.2 GPa,[35] respectively. Interestingly, our predicted ground-state $P\bar{4}2_1m$-WB has a hardness of 31.2 GPa, which is the highest hardness among the phases of the same composition. The stable $P2_1/m$-W_2B_3 phase, which we predicted, also has a high hardness of 31.7 GPa. The reported hardest stable structure is $P6_3/mmc$-$2u$-WB_2 with a hardness of 42.1 GPa. Strikingly, our predicted $Pmmn$-WB_5 is even harder; its hardness reaches 44.9 GPa. In a companion paper [Kvashnin *et al.*, 2018] we explore the W–B system at ambient pressure and non-zero temperatures.[36] There, we find that zero-point energy and vibrational entropy make this extraordinary new material thermodynamically stable and suitable for practical applications.

4 Conclusions

In summary, we have systematically investigated the stable and metastable crystal structures in the W–B system. Two novel stable phases, $P\bar{4}2_1m$-WB and $P2_1/m$-W_2B_3, and three nearly stable phases, $Ama2$-W_6B_5, $R3m$-W_2B_5, and $Pmmn$-WB_5, were first discovered at ambient pressure. Furthermore, our predictions show that the debated WB_4 becomes stable in the $P6_3/mmc$-$2u$ structure at the pressure of ~1 GPa. We present a complete phase diagram in the pressure range of 0–40 GPa and the newly discovered crystal structures. Important conclusions have been reached concerning the hardness of tungsten borides: (1) the newly-predicted $P\bar{4}2_1m$-WB displays a higher hardness than the previously-reported α and β phases. (2) $Pmmn$-WB_5 is the hardest tungsten boride. Our investigation provides a solid basis for the future synthesis of ultrahard tungsten boride materials.

Conflicts of interest

There are no conflicts to declare.

Acknowledgements

Y. Duan thanks the Fundamental Research Funds for the Central Universities (No. 2017XKZD08), the National Natural Science Foundation of China (No. 11774416), and the Provincial Natural Science Foundation of Jiangsu (No. BK20151138). H. Dong thanks the Guangdong National Science Funds for Distinguished Young Scholar (No. 2017B030306003). This work received financial support from LLC "Gazpromneft-STC" under a commercial contract with Skoltech entitled "Search for new superhard materials for drill bit cutters". We are grateful to the Advanced Analysis and Computation Center of CUMT for the award of CPU hours to accomplish this work.

References

1 R. B. Kaner, J. J. Gilman and S. H. Tolbert, *Science*, 2005, **308**, 1268.
2 V. V. Brazhkin, N. Dubrovinskaia, M. Nicol, N. Novikov, R. Riedel, V. Solozhenko and Y. Zhao, *Nat. Mater.*, 2004, **3**, 576.
3 V. L. Solozhenko and E. Gregoryanz, *Mater. Today*, 2005, **8**, 44.
4 Y. Tian, B. Xu, D. Yu, Y. Ma, Y. Wang, Y. Jiang, W. Hu, C. Tang, Y. Gao, K. Luo, Z. Zhao, L. M. Wang, B. Wen, J. He and Z. Liu, *Nature*, 2013, **493**, 385.
5 H. Y. Chung, M. B. Weinberger, J. B. Levine, A. Kavner, J. M. Yang, S. H. Tolbert and R. B. Kaner, *Science*, 2007, **316**, 436.
6 C. Lu, Q. Li, Y. Ma and C. F. Chen, *Phys. Rev. Lett.*, 2017, **119**, 115503.
7 R. Mohammadi, M. Xie, A. T. Lech, C. L. Turner, A. Kavner, S. H. Tolbert and R. B. Kaner, *J. Am. Chem. Soc.*, 2012, **134**, 20660.
8 A. G. Kvashnin, A. R. Oganov, A. I. Samtsevich and Z. Allahyari, *J. Phys. Chem. Lett.*, 2017, **8**, 755.
9 H. Gou, Z. Li, H. Niu, F. Gao, J. Zhang, R. C. Ewing and J. Lian, *Appl. Phys. Lett.*, 2012, **100**, 111907.
10 Q. Li, D. Zhou, W. Zheng, Y. Ma and C. F. Chen, *Phys. Rev. Lett.*, 2013, **110**, 136403.
11 X. Cheng, W. Zhang, X. Chen, H. Niu, P. Liu, K. Du, G. Liu, D. Li, H. Cheng, H. Ye and Y. Li, *Appl. Phys. Lett.*, 2013, **103**, 171903.
12 Q. Tao, D. Zheng, X. Zhao, Y. Chen, Q. Li, Q. Li, C. Wang, T. Cui, Y. Ma, X. Wang and P. Zhu, *Chem. Mater.*, 2014, **26**, 5297.
13 M. Wang, Y. Li, T. Cui, Y. Ma and G. Zou, *Appl. Phys. Lett.*, 2008, **93**, 101905.
14 Q. Gu, F. Krauss and W. Steurer, *Adv. Mater.*, 2008, **20**, 3620.

15 R. Mohammadi, A. T. Lech, M. Xie, B. E. Weaver, M. T. Yeung, S. H. Tolbert and R. B. Kaner, *Proc. Natl. Acad. Sci. U. S. A.*, 2011, **108**, 10958.
16 R. Kiessling, *Acta Chem. Scand.*, 1947, **1**, 893.
17 S. Okada, K. Kudou and T. Lundström, *Jpn. J. Appl. Phys.*, 1995, **34**, 226.
18 H. P. Woods, F. E. Wagner, Jr. and B. G. Fox, *Science*, 1966, **151**, 75.
19 Y. Liang, X. Yuan and W. Zhang, *Phys. Rev. B: Condens. Matter Mater. Phys.*, 2011, **83**, 220102(R).
20 R. F. Zhang, D. Legut, Z. J. Lin, Y. S. Zhao, H. K. Mao and S. Veprek, *Phys. Rev. Lett.*, 2012, **108**, 255502.
21 M. Frotscher, W. Klein, J. Bauer, C. M. Fang, J. F. Halet, A. Senyshyn, C. Baehtz and B. Albert, *Z. Anorg. Allg. Chem.*, 2007, **633**, 2626.
22 A. R. Oganov and C. W. Glass, *J. Chem. Phys.*, 2006, **124**, 244704.
23 A. R. Oganov, A. O. Lyakhov and M. Valle, *Acc. Chem. Res.*, 2011, **44**, 227.
24 A. O. Lyakhov, A. R. Oganov, H. T. Stokes and Q. Zhu, *Comput. Phys. Commun.*, 2013, **184**, 1172.
25 A. R. Oganov, J. Chen, C. Gatti, Y. Ma, Y. Ma, C. W. Glass, Z. Liu, T. Yu, O. O. Kurakevych and V. L. Solozhenko, *Nature*, 2009, **457**, 863.
26 Q. Zhu, D. Y. Jung, A. R. Oganov, C. W. Glass, C. Gatti and A. O. Lyakhov, *Nat. Chem.*, 2013, **5**, 61.
27 Y. Ma, M. Eremets, A. R. Oganov, Y. Xie, I. Trojan, S. Medvedev, A. O. Lyakhov, M. Valle and V. Prakapenka, *Nature*, 2009, **458**, 182.
28 J. P. Perdew, K. Burke and M. Ernzerhof, *Phys. Rev. Lett.*, 1996, **77**, 3865.
29 G. Kresse and J. Hafner, *Phys. Rev. B: Condens. Matter Mater. Phys.*, 1993, **47**, 558.
30 G. Kresse and J. Furthmuller, *Phys. Rev. B: Condens. Matter Mater. Phys.*, 1996, **54**, 11169.
31 G. Kresse and D. Joubert, *Phys. Rev. B: Condens. Matter Mater. Phys.*, 1999, **59**, 1758.
32 A. Togo, F. Oba and I. Tanaka, *Phys. Rev. B: Condens. Matter Mater. Phys.*, 2008, **78**, 134106.
33 X. Chen, H. Niu, D. Li and Y. Li, *Intermetallics*, 2011, **19**, 1275.
34 X. Cheng, X. Chen, D. Li and Y. Li, *Acta Crystallogr., Sect. C: Struct. Chem.*, 2014, **70**, 85.
35 Y. Liang, Z. Zhong and W. Zhang, *Comput. Mater. Sci.*, 2013, **68**, 222.
36 A. G. Kvashnin, H. A. Zakaryan, C. Zhao, Y. Duan, Y. A. Kvashnina, C. Xie, H. Dong and A. R. Oganov, *J. Phys. Chem. Lett.*, 2018, **9**, 3470.

